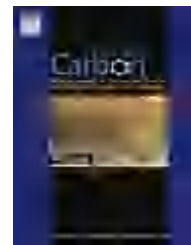


available at www.sciencedirect.comjournal homepage: www.elsevier.com/locate/carbon

Layered double hydroxides as catalysts for the efficient growth of high quality single-walled carbon nanotubes in a fluidized bed reactor

Meng-Qiang Zhao, Qiang Zhang *, Jia-Qi Huang, Jing-Qi Nie, Fei Wei *

Beijing Key Laboratory of Green Chemical Reaction Engineering and Technology, Department of Chemical Engineering, Tsinghua University, Beijing 100084, China

ARTICLE INFO

Article history:

Received 21 February 2010

Accepted 10 May 2010

Available online 15 May 2010

ABSTRACT

A family of layered double hydroxides (LDHs), such as Fe/Mg/Al, Co/Mg/Al, and Ni/Mg/Al LDHs, were used as catalysts for the efficient growth of single-walled carbon nanotubes (SWCNTs) in a fluidized bed reactor. The LDH flakes were agglomerated into clusters with sizes ranging from 50 to 200 μm , and they can be easily fluidized with a gas velocity ranging from 2.3 to 24 cm/s. After calcination and reduction, small metal catalyst particles formed and distributed uniformly on the flakes. At the reaction temperature, the introduction of methane realized the growth of SWCNTs with the diameter of 1–4 nm. The loose structure of LDH agglomerates afforded a yield as high as 0.95 $\text{g}_{\text{CNT}}/(\text{g}_{\text{cat}} \text{h})$ of SWCNTs with a surface area of 930 m^2/g . Compared with Fe/Mg/Al LDH, Ni/Mg/Al and Co/Mg/Al LDHs showed a better selectivity to SWCNTs. The highest selectivity for metallic SWCNTs was obtained using Co/Mg/Al LDHs as the catalyst.

© 2010 Elsevier Ltd. All rights reserved.

1. Introduction

Based on their unique structure, mechanical and electrical properties, single-walled carbon nanotubes (SWCNTs) have been explored for many potential applications in materials science, biology, electronics, and energy conversion/storage [1]. Controllable mass production of SWCNTs is the prerequisite for any large scale applications. In the past decade, many efforts have been made for low cost large scale synthesis of high purity SWCNTs. Various processes, such as arc discharge [2], floating catalyst process [3], high pressure carbon monoxide (HiPCO) process [4], and CoMoCat process [5], have been developed for this purpose. Catalysts are considered to play a crucial role in the processes mentioned above for the growth of CNTs. It is commonly accepted that the formation of small metal catalyst particles (0.5–5 nm) is the key factor

for the efficient growth of SWCNTs [3,4]. High dispersion of metal particles can be effectively achieved by using MgO [6–8] and SiO_2 [5] particles as the supports.

Up to now, the most efficient way for mass production of carbon nanotubes (CNTs) is fluidized-bed catalytic chemical vapor deposition (CVD) [9–12]. A pilot production of agglomerated multi-walled CNTs (MWCNTs) with high yield (15 kg/h) was achieved [13]. Agglomerated few-walled CNTs [14], SWCNTs [15], and aligned CNTs [16] have also been produced in a large scale in fluidized bed reactors. For SWCNT growth in a fixed bed reactor, impregnated, or co-precipitation catalysts, such as Fe/MgO, Co/Mo/ SiO_2 , were widely used as catalysts. However, due to the existence of a large amount of hydrogen in the fluidized bed reactor, the metal catalyst particles are still easy to sinter. This usually causes the formation of MWCNTs. The development of fluidizable catalysts

* Corresponding authors. Fax: +86 10 6277 2051.

E-mail addresses: zhang-qiang@mails.tsinghua.edu.cn (Q. Zhang), wf-dce@tsinghua.edu.cn (F. Wei).
0008-6223/\$ - see front matter © 2010 Elsevier Ltd. All rights reserved.
doi:10.1016/j.carbon.2010.05.019

for mass production of SWCNTs in a fluidized bed reactor that can avoid the sintering of small metal particles even with the existence of hydrogen is still a challenge.

Layered double hydroxides (LDHs), also known as hydroxide materials, are a class of synthetic two-dimensional nano-structured anionic clays, which consist of brucite-like layers. The divalent cations originally coordinated octahedrally by hydroxyl groups are isomorphously replaced by trivalent cations, affording the positively charged layers in the presence of charge-balancing anions. Hydrogen bonded water molecules may also occupy the remaining free space between layers. LDHs can be represented by the general formula $M_{1-x}^{2+}M_x^{3+}(\text{OH})_2A_{x/n}^{n-} \cdot m\text{H}_2\text{O}$, where M^{2+} ($M = \text{Fe}, \text{Co}, \text{Ni}, \text{Cu}, \text{Zn}, \text{Mg}$) and M^{3+} ($M = \text{Al}, \text{Cr}, \text{Ga}, \text{Mn}, \text{or Fe}$) are di- and trivalent cations, respectively; x is defined as the molar ratio of $M^{3+}/(M^{2+}+M^{3+})$ and generally with a value ranging from 0.2 to 0.33 [17]. Recently, the facile method for the controllable mass production of LDHs have been developed [17]. Numerous metals, such as Fe, Co, Ni, Cu, Zn, Mg, Al, and Ca, can be dispersed in the lamellar LDH flake at an atomic level with controllable component. This is contributed by the substitution of divalent metal cations by trivalent cations within the brucite-like layers. Compared with natural clay, the composition of LDHs is much simpler and can be controlled, which is of paramount importance for designing a catalyst, catalyst precursor and catalyst support. When LDH is calcined and reduced, metal particles can be formed and distributed uniformly on the calcined LDH flakes [18], which are good catalysts for the growth of CNTs. The sintering of small metal particles on LDH flakes

can be controlled. Recently, a few works have been published reporting on the in situ growth of CNTs on LDHs in a fixed bed reactor [19–21]. However, agglomerated MWCNTs with diameters ranging from 10 to 50 nm and a specific surface area of less than $50 \text{ m}^2/\text{g}$ were synthesized [19–21]. Recently, we have found that SWCNTs can be synthesized using LDHs as catalysts in a fixed bed reactor [18]. In this contribution, we report the efficient growth of SWCNTs on a family of LDHs in a fluidized bed reactor. High quality SWCNTs with a high surface area and low defect density were produced over the fluidizable calcined LDH flakes.

2. Experimental

2.1. Catalyst preparation

The Fe/Mg/Al LDH flakes were prepared using a urea assisted co-precipitation reaction. $\text{Mg}(\text{NO}_3)_2 \cdot 6\text{H}_2\text{O}$, $\text{Al}(\text{NO}_3)_3 \cdot 9\text{H}_2\text{O}$, and urea were dissolved in 250.0 mL deionized water with $[\text{Mg}^{2+}] + [\text{Al}^{3+}] = 0.15 \text{ mol/L}$, $n(\text{Mg}):n(\text{Al}) = 3:1$, $[\text{urea}] = 3.0 \text{ mol/L}$. $\text{Fe}(\text{NO}_3)_3 \cdot 9\text{H}_2\text{O}$ was then dissolved in the solution with molar ratio of Fe to Al of 0.4. The as-obtained solution was kept at 100°C under continuous magnetic stirring for 12 h in a flask (equipped with a reflux condenser) of 500.0 mL under ambient atmosphere. The obtained suspension was kept at 94°C for another 12 h without stirring. After filtering, washing and freeze-drying, the final products of brown-yellow powder were obtained. The other kinds of LDH flakes were prepared through the same process, of which the compositions were

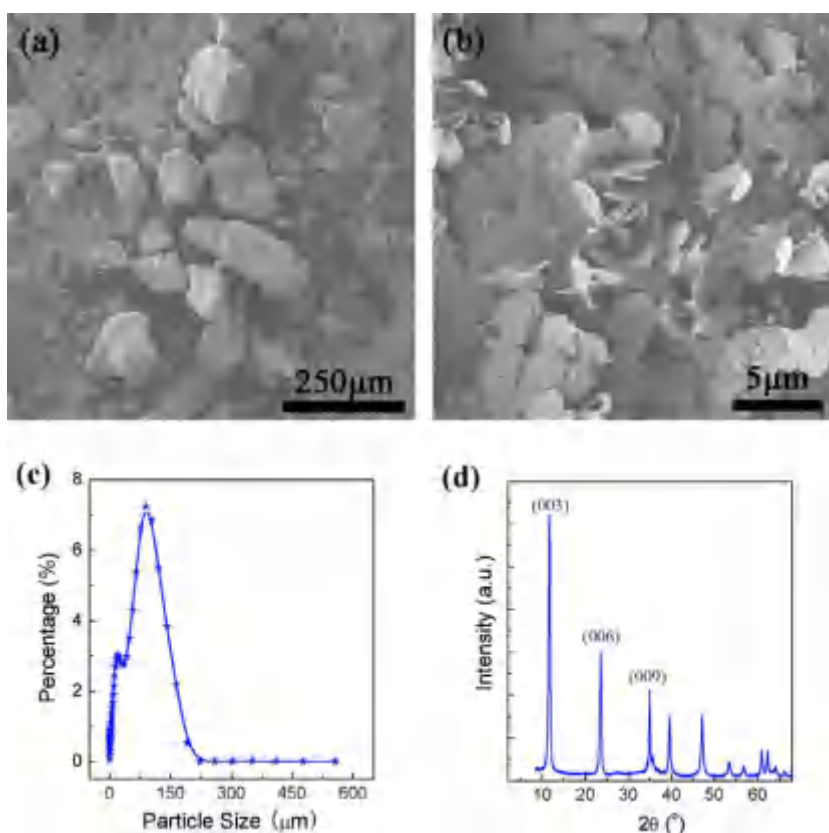


Fig. 1 – (a, b) The SEM images, (c) particle size distribution, and (d) XRD pattern of the Fe/Mg/Al LDH catalyst.

fixed as $n(\text{Co}):n(\text{Mg}):n(\text{Al}) = 0.4:3:1$, $n(\text{Ni}):n(\text{Mg}):n(\text{Al}) = 0.4:3:1$ and $n(\text{Co}):n(\text{Al}) = 2:1$.

2.2. SWCNT synthesis in a fluidized bed reactor

The apparatus used in the experiment is similar to that described in the previous report [22]. The fluidized bed reactor is made of quartz with an inner diameter of 20 mm and a height of 500 mm. A sintered porous plate is used as the gas distributor at the bottom of the reactor. The gas distributor also acts as the floor, which supports the solids in the reactor before they are suspended in gas flow. Here, the lamellar Fe/Mg/Al LDH flakes, as well as Co/Mg/Al, Ni/Mg/Al, and Co/Al LDH flakes were used as the catalysts. About 1.0 g catalyst was fed into the reactor before the reaction. The gas mixture containing carbon source entered the bottom vessel of the reactor and then passed through the gas distributor, the fluidized bed units, and finally flowed out. The quartz fluidized bed reactor, mounted in an electrical tube furnace, was heated to 900 °C in Ar atmosphere at a flow rate of 500 mL/min. The catalysts were pushed apart from one another due to the up-flow gas at a sufficient velocity. Once reaching the reaction temperature, H₂ with a flow rate of 50 mL/min was introduced into the reactor for the reduction. After 5 min, the flow rate of Ar was turned down to 100 mL/min and CH₄ (400 mL/min) was introduced into the fluidized bed, starting the reaction on the surface of the LDH flakes. Both the catalyst particles and the CNT products can be smoothly fluidized

in the reactor. After the reaction, the fluidized bed reactor was cooled down under Ar atmosphere. The as-grown products were then collected and characterized.

2.3. Characterizations

The size distributions of the suspended catalysts were obtained using particle characterization system (Malvern Mastersizer, Micro-plus). The reliability of the agglomerate size and the morphology of the LDH flakes were further confirmed by scanning electron microscope (SEM) observations. X-ray diffraction (XRD) patterns were recorded on a Rigaku D/max-RB diffractometer at 40.0 kV and 120 mA with Cu K α radiation. The Brunauer-Emmett-Teller (BET) specific surface area of all samples was measured by N₂ adsorption at liquid-N₂ temperature using Micromeritics Flow Sorb II 2300. Tests of H₂-temperature programmed reduction (TPR) of the LDH catalysts were conducted using a fixed-bed continuous-flow microreactor. To remove water vapor formed by the reduction of metallic oxide components of the catalyst sample, a KOH column and a 3A zeolite molecular sieve column were installed in sequence at the reactor exit. The ramp rate of temperature was 10 °C/min. Change of hydrogen signal was monitored by on-line GC (Shimadzu GC-8A) with a TCD detector. Fifty milligrams of LDH catalyst sample was first flushed by an Ar (of 99.999% purity, 20 sccm) stream at 673 K for 60 min to clean its surface, and then cooled down to room temperature, followed by switching to a N₂-carried 5.24 vol.%

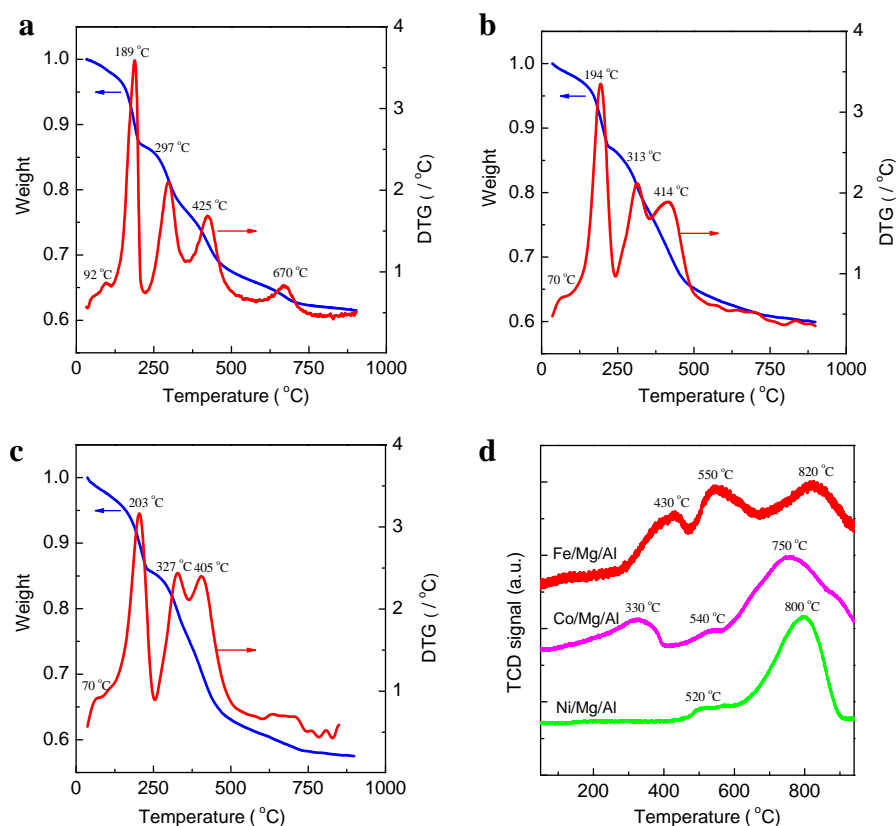


Fig. 2 - The TGA curves of the Fe/Mg/Al (a), Co/Mg/Al (b), and Ni/Mg/Al (c) LDH catalysts. (d) The TPR curves of the calcined Fe/Mg/Al, Co/Mg/Al and Ni/Mg/Al LDH catalysts.

H₂ gaseous mixture (20 sccm) as reducing gas to start the TPR observation. The fluidization characteristic of the LDH catalyst and as-grown products was investigated under ambient condition in an experimental apparatus as reported by Zhang et al. [22].

The morphology of the as-obtained SWCNTs was characterized using a JSM 7401F SEM operated at 3.0 kV, and a JEM 2010 high-resolution transmission electron microscope (TEM) operated at 120.0 kV. The sample for TEM observation was prepared using a common sonication method. Raman experiments were performed with a Renishaw RM2000 Raman spectrophotometer. The calcination process of LDHs and the purity of SWCNTs in the as-grown product were obtained through thermogravimetric analysis (TGA) by Q500.

3. Results and discussion

3.1. The LDH catalysts

Four kinds of LDHs with different compositions of Fe/Mg/Al, Co/Mg/Al, Ni/Mg/Al, and Co/Al LDHs were prepared as the catalysts for the synthesis of CNTs, respectively. Fe-based

catalyst has been extensively employed in the production of CNTs in fluidized bed reactors [12,13,16]. Compared with Ni/Co-based catalysts, Fe-based catalyst is much cheaper, which is of paramount importance for the large-scale production of CNTs. Thus, the Fe/Mg/Al LDH was selected as the model catalyst to study the morphological, structural, thermal, and reductive characteristics of LDH catalysts. After freeze-drying and scrunching, LDH agglomerates with particle sizes ranging from 50 to 200 μm were obtained, as shown in Fig. 1a. The SEM image from the Fe/Mg/Al LDH (Fig. 1b) reveals that the LDH flakes are 1–2 μm in size and tens of nanometers in thickness. The particle size distribution of the LDH agglomerates obtained from the particle characterization system is given in Fig. 1c. Typical powder XRD pattern for the as-prepared Fe/Mg/Al LDH is shown in Fig. 1d. The sharp and symmetric features of the diffraction peaks (0 0 3), (0 0 6), and (0 0 9) suggest that the as-produced LDH flakes have a high degree of crystallization. The diffraction peaks can be indexed as a rhombohedral structure with the refined lattice parameters of $a = 0.3043$ nm and $c = 2.2858$ nm for the Fe/Mg/Al LDH. Co/Mg/Al, Ni/Mg/Al and Co/Al LDHs showed similar morphologies and structures with the Fe/Mg/Al LDH.

Before the introduction of carbon source, the LDH catalysts needed to be calcined and reduced for the growth of CNTs. TGA and TPR were carried out to investigate the calcination and reduction behavior of the LDH catalysts. TGA of the as-prepared Fe/Mg/Al LDH catalyst under N₂ atmosphere shows five weight loss periods (Fig. 2a). The first weight loss period observed at around 92 °C with a weight loss of 2.0% in Fig. 2a can be attributed to the evaporation of free water existed in the LDH catalyst. A weight loss of 11.5% around 189 °C is resulted by the removal of physically adsorbed H₂O on the LDH flakes. When the temperature rises up to around 297 °C, the decomposition of CO₃²⁻ in the inter-layer spaces of LDH flake causes a weight loss of 10.0%. The fourth period with a weight loss of 13.2% appeared at around 425 °C can be explained by the decomposition of large amount of OH⁻ in the LDH flakes. The last weight loss of 2.5% observed at around 670 °C is thought to be the removal of residual OH⁻ and CO₃²⁻. TGA of Co/Mg/Al and Ni/Mg/Al LDHs were also carried out for comparison, and similar weight loss periods were observed, as shown in Fig. 2b and c. These findings are in good

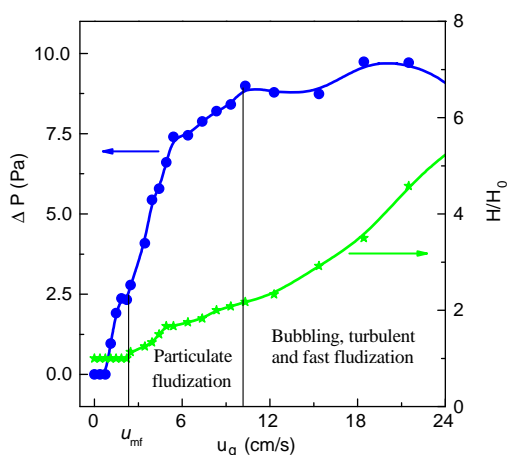


Fig. 3 – The fluidization characteristic of the Fe/Mg/Al LDH catalyst.

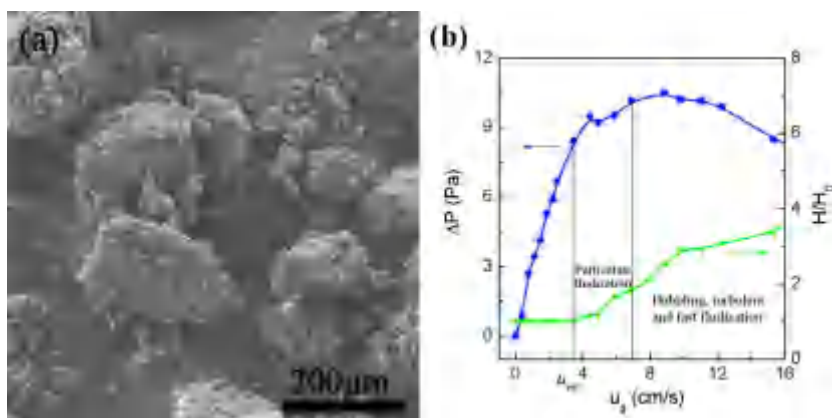


Fig. 4 – (a) SEM image of the as-grown products using Fe/Mg/Al LDH catalyst and (b) the fluidization characteristic of the as-grown products using Fe/Mg/Al LDH catalyst.

agreement of the thermal behaviors of various kinds of LDHs, such as Mg/Al-CO₃ [23], Co/Mg/Al-CO₃/NO₃ [24], Ni/Mg/Al-CO₃/NO₃ LDHs [24], reported in literatures.

Fig. 2d shows the TPR curves of the calcined Fe/Mg/Al, Co/Mg/Al and Ni/Mg/Al LDH catalysts. For Fe/Mg/Al LDH, the Fe atoms exist in Fe₂O₃ phase or MgFe₂O₄ spinel phase after the calcination [20]. During the reduction process, the Fe₂O₃ is reduced to Fe₃O₄, to FeO, and to Fe in the temperature ranges of 300–470, 470–600, and 600–700 °C, respectively [25]. The previous two reduction peaks are clearly shown in

Fig. 2d. Fe in MgFe₂O₄ spinel phase can be reduced at higher temperature (about 800–900 °C) [26]. For Co/Mg/Al LDH, the low temperature peaks around 330 °C and 540 °C correspond to the reduction of Co³⁺ to Co²⁺ and Co²⁺ to Co, respectively [27]. The high-temperature peak around 750 °C can be attributed to the reduction of the spinel phase (CoAl₂O₄) [24]. Similarly, for Ni/Mg/Al LDH, the peak around 520 °C can be assigned to the reduction of Ni²⁺ to Ni, while the peak around 800 °C can be attributed to the reduction of NiAl₂O₄ [24]. After the calcination and reduction, the morphology of

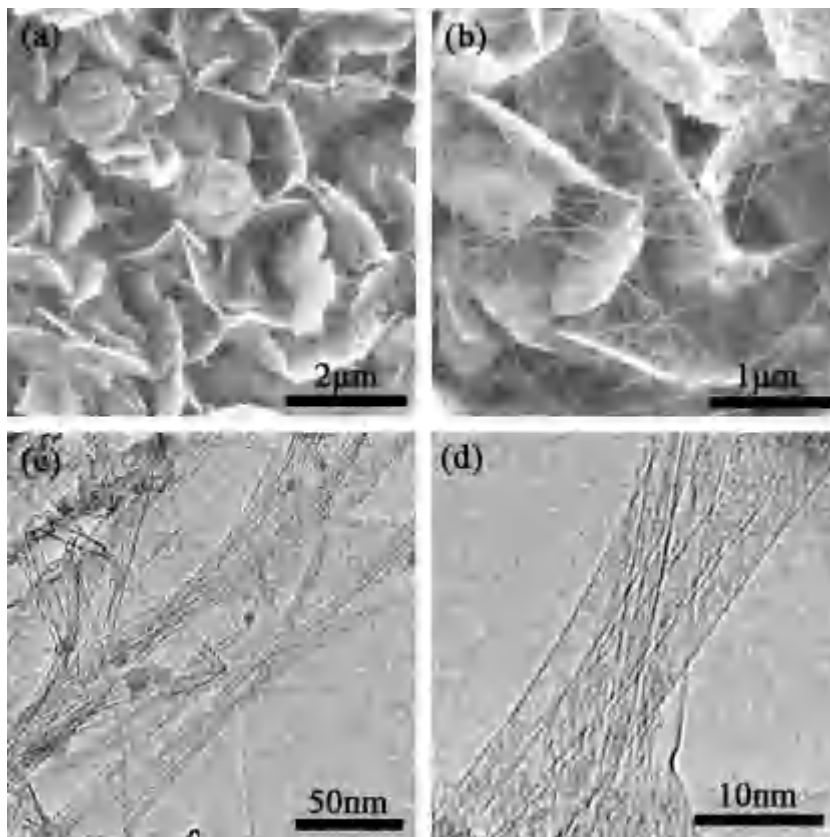


Fig. 5 - (a, b) SEM and (c, d) TEM images of the SWCNTs grown on Fe/Mg/Al LDH catalyst.

Table 1 - Comparison of the CNTs grown on various LDHs.

Catalyst	Products	Diameter (nm)	I _D /I _G ratio ^a	STY (g _{CNT} /(g _{cat} h)) ^b	Ref.
Co/Al-LDH	MWCNTs	25	1.1	1.3	[19,21,28]
Co/Fe/Al-LDH	MWCNTs	11	0.72	2.3	[30]
Ni/Mg/Al-LDH	MWCNTs	10	1.2	5.7	[31,32]
Fe/Mg/Al-LDH	SWCNTs	1.1	0.25	–	[20]
Fe/Zn/Al-LDH	MWCNTs	30	–	–	[20]
Co/Zn/Al-LDH	MWCNTs	14–30	–	0.1–0.2	[29]
Ni/Al-LDH	CNFs	200–700	0.79	–	[40]
Fe/Mg/Al-LDH	SWCNTs	1.0–6.0	0.06	0.95	This work
Co/Mg/Al-LDH	SWCNTs	1.0–3.0	0.09	–	
Ni/Mg/Al-LDH	SWCNTs	1.0–4.0	0.14	–	
Co/Al-LDH	S/MWCNTs	2.0–80	0.41	–	

^a The I_D/I_G ratio was obtained from the Raman spectra.

^b The space time yield (STY) of CNTs was obtained by TGA.

the obtained LDH flakes can be well preserved, and the as-obtained LDH agglomerates exhibited similar particle size distribution with that before the calcination and reduction.

3.2. Fluidization behavior of the catalyst and as-grown products

It is important to choose a proper operating gas velocity domain according to the fluidization behavior of the catalysts and the as-grown products. Fig. 3 shows the fluidization characteristic of the Fe/Mg/Al LDH catalyst. The intrinsic density

of the LDHs is ca. 2000 kg/m³, while the bulk density of the as-obtained LDH agglomerates after calcination and reduction is 380 kg/m³. According to the density and size distribution, the LDH agglomerates can be considered as A particles according to Geldart particle classification, exhibiting good fluidization behavior. Once the catalysts are exposed to an up-flow gas, the pressure drops and bed expansion raises when gas flow rate increases. The minimal fluidization velocity (u_{mf}) of the LDH catalyst is 2.3 cm/s. The catalyst is then in fluidized state when the gas velocity is over u_{mf} . Several flow regimes are identified as particulate fluidization, bubbling

Table 2 – Comparison of the quality of SWCNTs grown on various catalysts.

Catalyst	Products	Diameter (nm)	I_D/I_G ratio ^a	STY (g _{CNT} /(g _{cat} h)) ^b	Ref.
Fe(CO) ₅	SWCNTs	0.9	–	0.079	[4]
Co/Mo/SiO ₂	SWCNTs	0.9	0.05	0.30	[5]
Ferrocene	S/MWCNTs	2.0	–	8.0	[3]
Fe/MgO	SWCNTs	1–3	0.06–0.2	0.30	[41]
Fe/Mg/Al/O	DWCNTs	1.7–3.0	0.2	0.15–0.25	[42]
Fe/Mo/MgO	S/MWCNTs	1–10	0.1–0.4	–	[43]
Fe/Mg/Al-LDH	SWCNTs	1.0–6.0	0.06	0.95	This work
Co/Mg/Al-LDH	SWCNTs	1.0–3.0	0.09	–	

^a The I_D/I_G ratio was obtained from the Raman spectra.

^b The STY of CNTs was obtained by TGA.

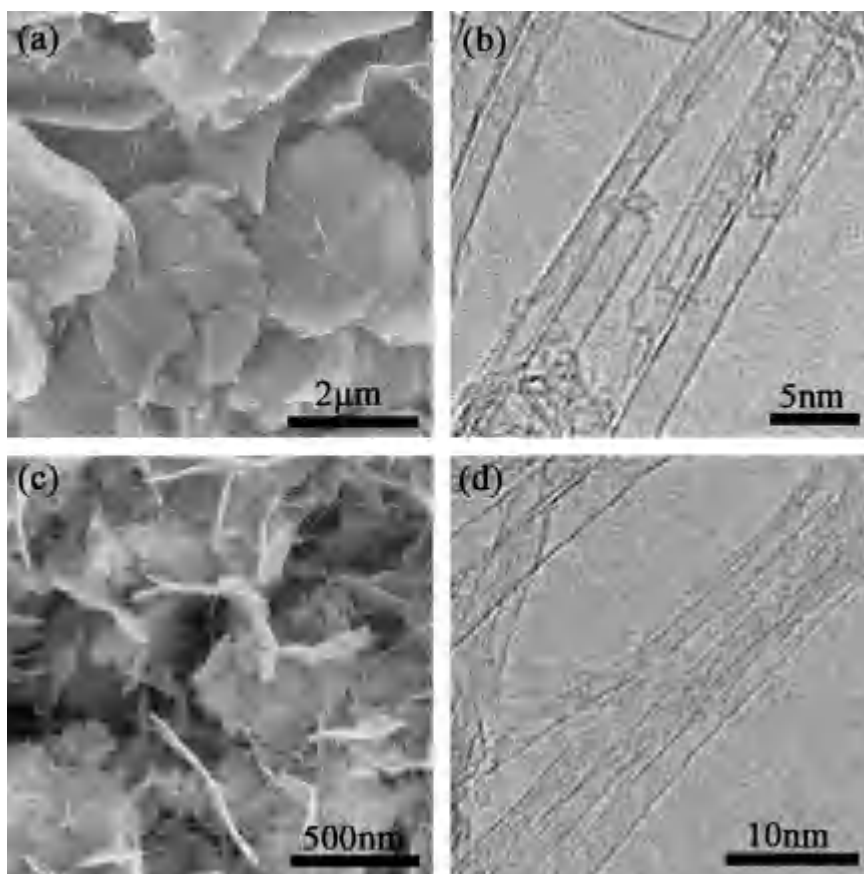


Fig. 6 – (a) SEM and (b) TEM image of the SWCNTs grown on Co/Mg/Al LDH catalyst; (c) SEM and (d) TEM image of the SWCNTs grown on Ni/Mg/Al LDH catalyst.

fluidization, and turbulent fluidization with an increasing gas velocity. The pressure drop tends to be stable when the gas velocity is larger than 10.1 cm/s, indicating the beginning of bubbling fluidization. If the gas velocity further increases, turbulent fluidization, fast fluidization, and the pneumatic conveying regimes will be achieved. It is concluded that the stable fluidization state of the LDH catalyst can be maintained within a large gas velocity domain from 10.1 to 22.0 cm/s.

After the growth of CNTs, the size of the as-grown particles expanded to ca. 200 μm , as shown in Fig. 4a. The fluidization curve of the as-grown particles is shown in Fig. 4b. Compared with pristine LDH catalysts, the as-grown products are with slightly larger u_{mf} of 3.1 cm/s and smaller bubbling fluidization beginning gas velocity of 7.0 cm/s due to the larger particle size and smaller bulk density induced by the growth of CNTs. Therefore, the gas velocity was kept at about 11.4 cm/s in the reactor to ensure a good fluidization state during the whole CNT synthesis process.

3.3. As-grown SWCNTs in the fluidized bed reactor

CH_4 was introduced into the fluidized bed reactor after the calcination and reduction process. Typical morphology of the as-obtained products is shown in Fig. 5a and b. It can be observed that with short growth duration, large amount of CNTs were produced among the Fe/Mg/Al LDH flakes. TEM images of the products shown in Fig. 5c and d indicate that the as-grown CNTs in the fluidized bed reactor were mainly SWCNTs.

We compare the structures and properties of the CNTs obtained in the present work with those reported by other groups. In literatures, mainly MWCNTs with much larger diameter and higher I_D/I_G ratio were usually obtained when using different LDHs as catalysts (Table 1), such as Co/Al, Co/Fe/Al, Ni/Mg/Al, Fe/Zn/Al LDHs [19–21,28–32]. MWCNTs could also be easily synthesized on various natural catalysts, such as montmorillonites [33], bentonites [34], vermiculites [35], lavas [36,37], and sands [38,39]. Zhao et al. successfully synthesized SWCNTs with small diameter of 1.1 nm using Fe/Mg/Al LDH in a fixed bed reactor [20]. Here, the SWCNTs produced on Fe/Mg/Al LDH catalysts in a fluidized bed reactor are with high quality and large yield (Table 1). They have a mean diameter of 3.0 nm and a specific surface area of 930 m^2/g . The quality of the SWCNTs grown on LDH flakes in fluidized bed was also competitive with those obtained by other methods (Table 2) [3–5,41–43]. Compared with CNTs synthesized using Fe/MgO [41], Fe/Mg/Al/O [42], and Fe/Mo/MgO [43] catalysts, the SWCNTs obtained on Fe/Mg/Al LDH catalyst are with much lower I_D/I_G ratio and higher yield though they are with similar diameter distribution. Though CNTs growth by the floating catalyst methods exhibits a high yield of CNTs [3], the purity of the as-obtained SWCNTs is low and the content of impurities, which are mainly composed of MWCNTs and amorphous carbon, can be as high as 40%.

SWCNTs can also be effectively synthesized on Co/Mg/Al and Ni/Mg/Al LDHs (Fig. 6). However, it is difficult to synthesize SWCNTs with high quality on Co/Al LDHs. The SEM images of the products obtained on Co/Al LDH were shown

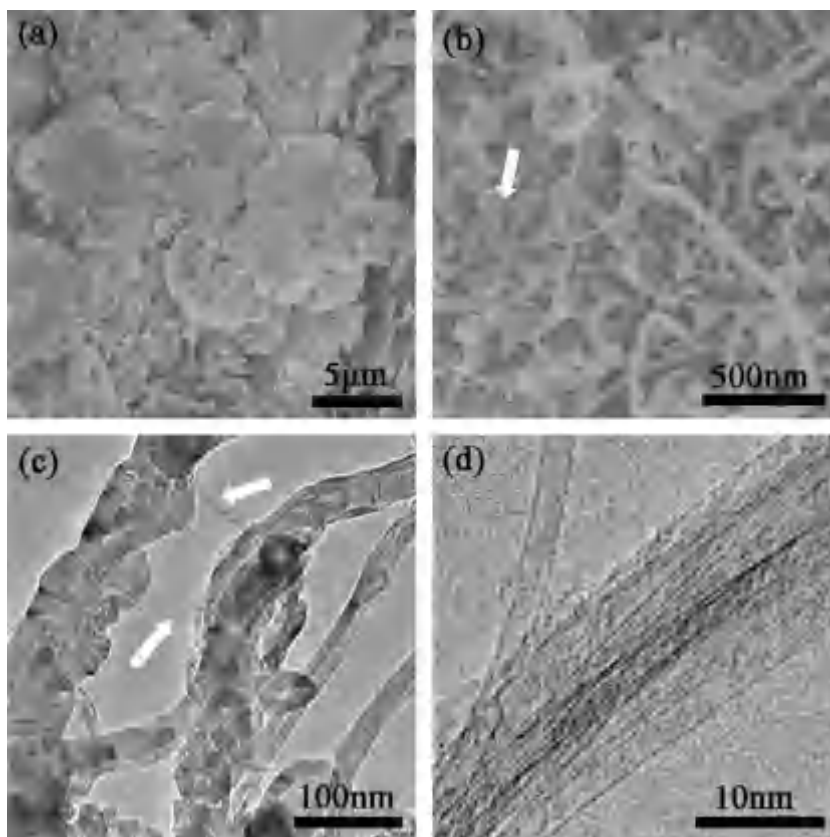


Fig. 7 – (a, b) SEM and (c, d) TEM images of the CNTs grown on Co/Al LDH catalyst.

in Fig. 7a and b. It is noticed that the plate-like morphology of the LDH flake is detrimentally damaged into flakes with irregular shape, on which CNTs with large diameters can be found. Fig. 7c reveals that the as-grown CNTs were mainly composed of MWCNTs with a high defect density. Only small bundles of SWCNTs (Fig. 7d) can also be found in both the SEM and TEM images, as indicated by the white arrows in Fig. 7b and c.

The diameter and wall number distributions of CNTs grown on Fe(Co, Ni)/Mg/Al LDHs were obtained by measuring around 200 individual CNTs on high-resolution TEM images.

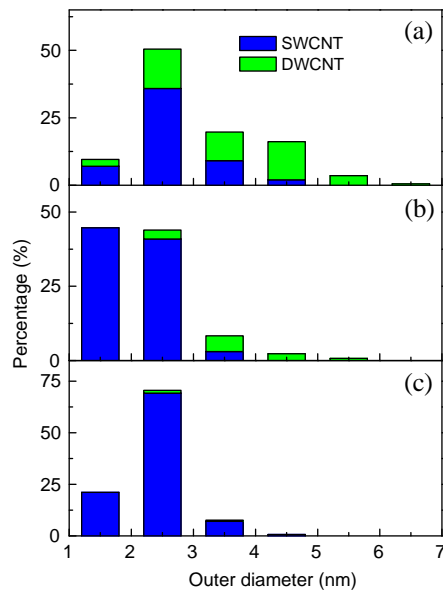


Fig. 8 – Wall number and diameter distribution of the CNTs on different LDH catalysts: (a) Fe/Mg/Al; (b) Co/Mg/Al and (c) Ni/Mg/Al.

As shown in Fig. 8, when Fe/Mg/Al LDH was used as the catalyst, 54.0% of the as-obtained CNTs corresponded to SWCNTs with diameters ranging from 1.0 to 5.0 nm. The others were double walled carbon nanotubes (DWCNTs) with diameters distributed from 1.0 to 6.0 nm and few MWCNTs were found. The proportion of DWCNTs decreased significantly to 11.4% when Co/Mg/Al LDH was used as catalyst. The diameter of the as-obtained SWCNTs also decreased to a range from 1.0 to 3.0 nm. Ni/Mg/Al LDH catalyst exhibited higher selectivity to SWCNTs with the proportion of DWCNTs as low as 1.9%, and the diameters of SWCNTs were with similar distribution with that of Fe/Mg/Al LDH. Thus, it is concluded that both the wall number and diameter of the obtained CNTs can be tuned by changing the composition of LDHs.

Raman spectra of the as-obtained SWCNTs on Fe/Mg/Al LDH excited by lasers with different wavelength (488, 514, 633, 785 nm) were recorded. Fig. 9a shows the radial breathing mode (RBM) peaks for the SWCNTs grown on Fe/Mg/Al LDH catalyst, and the Kataura plot [44,45] directly showing the regions of metallic (blue spots) and semiconducting (black spots) nanotubes is attached as well. No RBM peak can be found in the Raman spectra excited by the 488 wavelength laser. In the Raman spectra excited by the 514 wavelength laser, typical RBM features for semiconducting nanotubes in the region of 122–184 cm^{-1} are illustrated. There are still special features at around 119 and 258 cm^{-1} , which confirmed the existence of metallic nanotubes. When the CNTs grown on Fe/Mg/Al LDH are excited by the 633 nm wavelength laser, the RBM peaks at around 190 and 218 cm^{-1} are much stronger, indicating there are more metallic nanotubes showing Raman activity at this wavelength. The ratio of metallic to semi-conductive bands is estimated to be about 2:5 for 514 nm wavelength laser and 3:1 for 633 nm wavelength laser, according to the integral intensities of the relative peaks. The

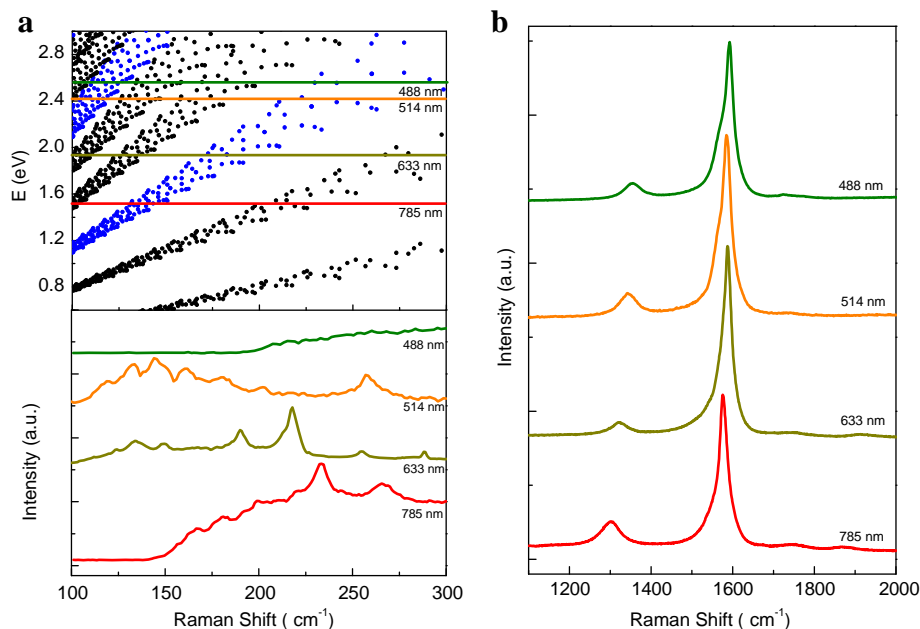


Fig. 9 – Raman spectra of the as-obtained SWCNTs on Fe/Mg/Al-LDH excited with 488, 514, 633, and 785 nm lasers: (a) RBM peaks and (b) D and G peaks.

RBM mode recorded with a 785 nm laser shows extensive signals of semiconducting nanotubes as only semiconducting nanotubes are Raman active at this particular excitation wavelength [46]. For the SWCNTs grown on Co/Mg/Al and Ni/Mg/Al LDHs, RBM peaks are also found in the Raman spectra excited with 633 nm laser (Fig. 10a). However, the number of the RBM peaks decreases significantly, indicating the concentrated diameter distribution and the increasing content of SWCNTs. Besides, it is observed that the intensity of peaks at higher wave number (190, 213 cm^{-1}) for SWCNTs on Co/Mg/Al LDHs are much stronger than that on Ni/Mg/Al LDHs, indicating that the SWCNTs on Co/Mg/Al LDHs are of smaller diameters, which is in good agreement with the diameter distribution shown in Fig. 8. The ratios of the integral intensities of RBM features for semiconducting nanotubes to those for metallic nanotubes are 0.23, 1.1 and 0.34 for SWCNTs grown on Co/Mg/Al, Ni/Mg/Al and Fe/Mg/Al LDHs, respectively. This indicates that Co/Mg/Al LDHs exhibit the highest selectivity to metallic nanotubes [47,48]. The preferential growth of SWCNTs is still an issue to be explored. The values of I_D/I_G for SWCNTs on Fe/Mg/Al, Co/Mg/Al and Ni/Mg/Al LDH are 0.06, 0.09 and 0.14, respectively (Figs. 9b, 10b and Table 1). The low I_D/I_G value indicates that the as-obtained SWCNTs are all of high quality.

Up to now, it has been demonstrated that Fe/Mg/Al LDH, as well as Co/Mg/Al and Ni/Mg/Al LDHs are good catalysts for the efficient growth of SWCNTs in fluidized bed. The fluidized bed has great advantages in terms of enough growth space, excellent diffusion and heat transfer, easiness in scaling up and continuous operation for CNT production [9–13,16,49–51]. The metal particles with high density and good dispersion can be easily modulated by the composition of LDH catalysts, which are quite important to modulate the structure of CNTs. Based on the extensive strategies for growth, SWCNTs with high surface area and good graphitization can be produced in large scale to facilitate the applications in the area of composites, fuel cells, supercapacitors, lithium ion secondary batteries, and energy absorbing materials [1,33–36,52].

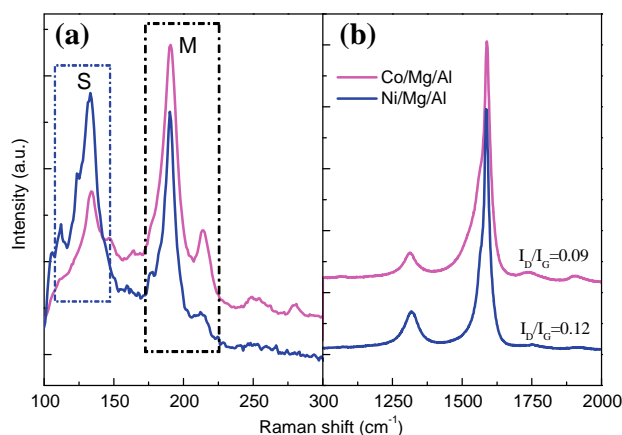


Fig. 10 – Raman spectra of the as-obtained SWCNTs on Co/Mg/Al and Ni/Mg/Al LDHs excited with 633 nm laser: (a) RBM peaks and (b) D and G peaks.

4. Conclusions

Efficient growth of high quality SWCNTs was achieved by fluidized-bed CVD using Fe/Mg/Al, Co/Mg/Al and Ni/Mg/Al LDHs as the catalysts. The LDH flakes exhibited good fluidization characteristics due to the agglomeration caused by van der Waals interaction. Large amount of SWCNTs with diameters of 1–4 nm can be synthesized on the surface of LDH flakes due to the loose structure of LDH agglomerates. Co/Mg/Al and Ni/Mg/Al LDHs gave a better selectivity to SWCNT synthesis compared with Fe/Mg/Al LDH catalyst, and the Co/Mg/Al LDH exhibited the best selectivity to metallic SWCNTs based on the results of Raman spectra. Large-scale production of SWCNTs with high surface area and good graphitization can be achieved on LDH flakes in fluidized bed reactor for further applications in the area of composites, energy conversion, catalysis, and devices.

Acknowledgements

The work was supported by the Foundation for the Natural Scientific Foundation of China (No. 20736004, No. 20736007, No. 2007AA03Z346), the China National Program (No. 2006CB0N0702). The authors thank Prof. S. Maruyama, Dr. K. Sato, and Dr. R. Xiang greatly for providing the Kataura plot data and Prof. D.S. Su for helpful discussion.

REFERENCES

- [1] Zhou WY, Bai XD, Wang EG, Xie SS. Synthesis, structure, and properties of single-walled carbon nanotubes. *Adv Mater* 2009;21(45):4565–83.
- [2] Journet C, Maser WK, Bernier P, Loiseau A, delaChapelle ML, Lefrant S, et al. Large-scale production of single-walled carbon nanotubes by the electric-arc technique. *Nature* 1997;388(6644):756–8.
- [3] Cheng HM, Li F, Su G, Pan HY, He LL, Sun X, et al. Large-scale and low-cost synthesis of single-walled carbon nanotubes by the catalytic pyrolysis of hydrocarbons. *Appl Phys Lett* 1998;72(25):3282–4.
- [4] Nikolaev P, Bronikowski MJ, Bradley RK, Rohmund F, Colbert DT, Smith KA, et al. Gas-phase catalytic growth of single-walled carbon nanotubes from carbon monoxide. *Chem Phys Lett* 1999;313(1–2):91–7.
- [5] Irurzun VM, Tan YQ, Resasco DE. Sol-gel synthesis and characterization of Co-Mo/silica catalysts for single-walled carbon nanotube production. *Chem Mater* 2009;21(11):2238–46.
- [6] Li QW, Yan H, Cheng Y, Zhang J, Liu ZF. A scalable CVD synthesis of high-purity single-walled carbon nanotubes with porous MgO as support material. *J Mater Chem* 2002;12(4):1179–83.
- [7] Wang Y, Liu YQ, Wei DC, Cao LC, Fu L, Li XL, et al. Controlled growth of single-walled carbon nanotubes at atmospheric pressure by catalytic decomposition of ethanol and an efficient purification method. *J Mater Chem* 2007;17(4):357–63.
- [8] Ago H, Imamura S, Okazaki T, Saitoj T, Yumura M, Tsuji M. CVD growth of single-walled carbon nanotubes with narrow diameter distribution over Fe/MgO catalyst and their fluorescence spectroscopy. *J Phys Chem B* 2005;109(20):10035–41.

- [9] Philippe R, Moranqais A, Corrias M, Caussat B, Kihn Y, Kalck P, et al. Catalytic production of carbon nanotubes by fluidized-bed CVD. *Chem Vapor Depos* 2007;13(9):447–57.
- [10] See CH, Harris AT. A review of carbon nanotube synthesis via fluidized-bed chemical vapor deposition. *Ind Eng Chem Res* 2007;46(4):997–1012.
- [11] Wei F, Zhang Q, Qian WZ, Yu H, Wang Y, Luo GH, et al. The mass production of carbon nanotubes using a nano-agglomerate fluidized bed reactor: a multiscale space-time analysis. *Powder Technol* 2008;183(1):10–20.
- [12] Danafar F, Fakhru'l-Razi A, Salleh MAM, Biak DRA. Fluidized bed catalytic chemical vapor deposition synthesis of carbon nanotubes – a review. *Chem Eng J* 2009;155(1–2):37–48.
- [13] Wang Y, Wei F, Luo GH, Yu H, Gu GS. The large-scale production of carbon nanotubes in a nano-agglomerate fluidized-bed reactor. *Chem Phys Lett* 2002;364(5–6):568–72.
- [14] Zhang Q, Yu H, Liu Y, Qian WZ, Wang Y, Luo GH, et al. Few walled carbon nanotube production in large-scale by nano-agglomerate fluidized-bed process. *Nano* 2008;3(1):45–50.
- [15] Li YL, Kinloch IA, Shaffer MS, Geng JF, Johnson B, Windle AH. Synthesis of single-walled carbon nanotubes by a fluidized-bed method. *Chem Phys Lett* 2004;384(1–3):98–102.
- [16] Zhang Q, Zhao MQ, Huang JQ, Nie JQ, Wei F. Mass production of aligned carbon nanotube arrays grown on clay by fluidized bed catalytic chemical vapor deposition. *Carbon* 2010;48(4):1196–209.
- [17] Evans DG, Duan X. Preparation of layered double hydroxides and their applications as additives in polymers, as precursors to magnetic materials and in biology and medicine. *Chem Commun* 2006(5):485–96.
- [18] Zhao MQ, Zhang Q, Jia XL, Huang JQ, Zhang YH, Wei F. Hierarchical composites of single/double walled carbon nanotubes interlinked flakes from direct carbon deposition on layered double hydroxides. *Adv Funct Mater* 2010;28(4):677–95.
- [19] Li F, Tan Q, Evans DG, Duan X. Synthesis of carbon nanotubes using a novel catalyst derived from hydrotalcite-like Co–Al layered double hydroxide precursor. *Catal Lett* 2005;99(3–4):151–6.
- [20] Zhao Y, Jiao QZ, Li CH, Liang J. Catalytic synthesis of carbon nanostructures using layered double hydroxides as catalyst precursors. *Carbon* 2007;45(11):2159–63.
- [21] Hima HI, Xiang X, Zhang L, Li F. Novel carbon nanostructures of caterpillar-like fibers and interwoven spheres with excellent surface super-hydrophobicity produced by chemical vapor deposition. *J Mater Chem* 2008;18(11):1245–52.
- [22] Zhang Q, Zhao MQ, Huang JQ, Liu Y, Wang Y, Qian WZ, et al. Vertically aligned carbon nanotube arrays grown on a lamellar catalyst by fluidized bed catalytic chemical vapor deposition. *Carbon* 2009;47(11):2600–10.
- [23] Yang WS, Kim Y, Liu PKT, Sahimi M, Tsotsis TT. A study by in situ techniques of the thermal evolution of the structure of a Mg–Al–CO₃ layered double hydroxide. *Chem Eng Sci* 2002;57(15):2945–53.
- [24] Chmielarz L, Kustrowski P, Rafalska-Lasocha A, Dziembaj R. Influence of Cu, Co and Ni cations incorporated in brucite-type layers on thermal behaviour of hydrotalcites and reducibility of the derived mixed oxide systems. *Thermochim Acta* 2003;395(1–2):225–36.
- [25] Munteanu G, Ilieva L, Andreeva D. Kinetic parameters obtained from TPR data for a-Fe₂O₃ and Au/a-Fe₂O₃ systems. *Thermochim Acta* 1997;291(1–2):171–7.
- [26] Fernandez JM, Ulibarri MA, Labajos FM, Rives V. The effect of iron on the crystalline phases formed upon thermal decomposition of Mg–Al–Fe hydrotalcites. *J Mater Chem* 1998;8(11):2507–14.
- [27] Wang B, Yang Y, Li LJ, Chen Y. Effect of different catalyst supports on the (n, m) selective growth of single-walled carbon nanotube from Co–Mo catalyst. *J Mater Sci* 2009;44(12):3285–95.
- [28] Hima HI, Xiang X, Zhang L, Li F, Evans DG. Influence of cobalt content on structure and composition of calcined Co–Al layered double hydroxides and catalytic property for the carbon nanotubes formation. *Chinese J Inorg Chem* 2008;24(6):886–91.
- [29] Benito P, Herrero M, Labajos FM, Rives V, Royo C, Latorre N, et al. Production of carbon nanotubes from methane use of Co–Zn–Al catalysts prepared by microwave-assisted synthesis. *Chem Eng J* 2009;149(1–3):455–62.
- [30] Xiang X, Zhang L, Hima HI, Li F, Evans DG. Co-based catalysts from Co/Fe/Al layered double hydroxides for preparation of carbon nanotubes. *Appl Clay Sci* 2009;42(3–4):405–9.
- [31] Zhao Y, Jiao QZ, Liang J, Li CH. Synthesis of Ni/Mg/Al layered double hydroxides and their use as catalyst precursors in the preparation of carbon nanotubes. *Chem Res Chinese U* 2005;21(4):471–5.
- [32] Zhang L, Li F, Xiang X, Wei M, Evans DG. Ni-based supported catalysts from layered double hydroxides: tunable microstructure and controlled property for the synthesis of carbon nanotubes. *Chem Eng J* 2009;155(1–2):474–82.
- [33] Zhang WD, Phang IY, Liu TX. Growth of carbon nanotubes on clay: unique nanostructured filler for high-performance polymer nanocomposites. *Adv Mater* 2006;18(1):73–7.
- [34] Rinaldi A, Zhang J, Mizera J, Girgsdies F, Wang N, Hamid SBA, et al. Facile synthesis of carbon nanotube/natural bentonite composites as a stable catalyst for styrene synthesis. *Chem Commun* 2008(48):6528–30.
- [35] Zhang Q, Zhao MQ, Liu Y, Cao AY, Qian WZ, Lu YF, et al. Energy-absorbing hybrid composites based on alternate carbon-nanotube and inorganic layers. *Adv Mater* 2009;21(28):2876–80.
- [36] Su DS, Chen XW, Liu X, Delgado JJ, Schlogl R, Gajovic A. Mount-etna-lava-supported nanocarbons for oxidative dehydrogenation reactions. *Adv Mater* 2008;20(19):3597–600.
- [37] Su DS, Chen XW. Natural lavas as catalysts for efficient production of carbon nanotubes and nanofibers. *Angew Chem Int Ed* 2007;46(11):1823–4.
- [38] Endo M, Takeuchi K, Kim YA, Park KC, Ichiki T, Hayashi T, et al. Simple synthesis of multiwalled carbon nanotubes from natural resources. *ChemSusChem* 2008;1(10):820–2.
- [39] Su DS. The use of natural materials in nanocarbon synthesis. *ChemSusChem* 2009;2(11):1009–20.
- [40] Zhang L, Zhang CF, Xiang X, Li F. Synthesis of novel submicrometer-scale flat carbon fibers and application in the electrooxidation of methanol. *Chem Eng Technol* 2010;33(1):44–51.
- [41] Wen Q, Qian WZ, Wei F, Liu Y, Ning GQ, Zhang Q. CO₂-assisted SWNT growth on porous catalysts. *Chem Mater* 2007;19(6):1226–30.
- [42] Zhang Q, Qian WZ, Wen Q, Liu Y, Wang DH, Wei F. The effect of phase separation in Fe/Mg/Al/O catalysts on the synthesis of DWCNTs from methane. *Carbon* 2007;45(8):1645–50.
- [43] Yu H, Zhang Q, Zhang QF, Wang QX, Ning GQ, Luo GH, et al. Effect of the reaction atmosphere on the diameter of single-walled carbon nanotubes produced by chemical vapor deposition. *Carbon* 2006;44(9):1706–12.
- [44] Kataura H, Kumazawa Y, Maniwa Y, Umezumi I, Suzuki S, Ohtsuka Y, et al. Optical properties of single-wall carbon nanotubes. *Synthetic Met* 1998;103(1–3):2555–8.
- [45] Jorio A, Araujo PT, Doorn SK, Maruyama S, Chacham H, Pimenta MA. The Kataura plot over broad energy and diameter ranges. *Phys Status Solidi B* 2006;243(13):3117–21.

- [46] Zheng M, Jagota A, Strano MS, Santos AP, Barone P, Chou SG, et al. Structure-based carbon nanotube sorting by sequence-dependent DNA assembly. *Science* 2003;302(5650):1545–8.
- [47] Harutyunyan AR, Chen GG, Paronyan TM, Pigos EM, Kuznetsov OA, Hewaparakrama K, et al. Preferential growth of single-walled carbon nanotubes with metallic conductivity. *Science* 2009;326(5949):116–20.
- [48] Hong G, Zhang B, Peng BH, Zhang J, Choi WM, Choi JY, et al. Direct growth of semiconducting single-walled carbon nanotube array. *J Am Chem Soc* 2009;131(41):14642–3.
- [49] Morancais A, Caussat B, Kihn Y, Kalck P, Plee D, Gaillard P, et al. A parametric study of the large scale production of multi-walled carbon nanotubes by fluidized bed catalytic chemical vapor deposition. *Carbon* 2007;45(3):624–35.
- [50] See CH, Harris AT. A comparison of carbon nanotube synthesis in fixed and fluidised bed reactors. *Chem Eng J* 2008;144(2):267–9.
- [51] Liu XB, Sun H, Chen Y, Lau R, Yang YH. Preparation of large particle MCM-41 and investigation on its fluidization behavior and application in single-walled carbon nanotube production in a fluidized-bed reactor. *Chem Eng J* 2008;142(3):331–6.
- [52] Su DS, Schlogl R. Nanostructured carbon and carbon nanocomposites for electrochemical energy storage applications. *ChemSusChem* 2010;3(2):136–68.